3) 厚生労働省：蛍光染色による細菌数の迅速測定法．第十五改正日本薬局方第二追補，東京，pp.228-230（2009）〔http://jpdb.nihs.go.jp/jp15supp2/〕
4) Rodriguez GG, *et al.*, Use of a fluorescent redox probe for direct visualization of actively respiring bacteria. *Appl Environ Microbiol*, 58: 1801-1808（1992）
5) Yamaguchi N, *et al.*, Rapid in situ enumeration of physiologically active bacteria in river waters using fluorescent probes. *Microbes Environ*, 12: 1-8（1997）
6) 邑瀬章文 他：蛍光染色法による地下水中の細菌数の迅速な測定．防菌防黴誌，27: 785-792（1999）
7) Kawai M, *et al.*, Rapid enumeration of physiologically active bacteria in purified water used in the pharmaceutical manufacturing process. *J Appl Microbiol*, 86: 496-504（1999）
8) 仲島道子 他：蛍光活性染色法を用いた紫外線殺菌水の衛生微生物学的評価．防菌防黴誌，26: 245-249（1998）
9) 谷佳津治 他：活性染色法による香辛料中の細菌の迅速な検出．防菌防黴誌，26: 415-421（1998）
10) Nakajima K, *et al.*, Rapid monitoring of microbial contamination on herbal medicines by fluorescent staining method. *Lett Appl Microbiol*, 40: 128-132（2005）
11) Kaeberlein T, *et al.*, Isolating "uncultivable" microorganisms in pure culture in a simulated natural environment. *Science*, 296: 1127-1129（2002）
12) DeLong EF, *et al.*, Phylogenetic stains: ribosomal RNA-based probes for the identification of single cells. *Science*, 243: 1360-1363（1989）
13) Amann RI, *et al.*, Fluorescent-oligonucleotide probing of whole cells for determinative, phylogenetic, and environmental studies in microbiology. *J Bacteriol*, 172: 762-770（1990）
14) Yamaguchi N, *et al.*, Selective enumeration of viable Enterobacteriaceae and *Pseudomonas* spp. in milk within 7h by multicolor fluorescence in situ hybridization following microcolony formation. *J Biosci Bioeng*, 113: 746-750（2012）
15) Kitaguchi A, *et al.*, Enumeration of respiring *Pseudomonas* spp. in milk within six hours by fluorescence in situ hybridization following formazan reduction. *Appl Environ Microbiol*, 71: 2748-2752（2005）
16) Muyzer G, *et al.*, Profiling of complex microbial populations by denaturing gradient gel electrophoresis analysis of polymerase chain reaction-amplified genes coding for 16S rRNA. *Appl Environ Microbiol*, 59: 695-700（1993）
17) Iwamoto T, *et al.*, Monitoring impact of in situ biostimulation treatment on groundwater bacterial community by DGGE. *FEMS Microbiol Ecol*, 32: 129-141（2000）
18) Tani K, *et al.*, Dynamics of methanotrophs during in situ bioremediation. *Microbes Environ*, 16: 37-42（2001）
19) Kawai M, *et al.*, 16S ribosomal DNA-based analysis of bacterial diversity in purified water used in pharmaceutical manufacturing processes by PCR and denaturing gradient gel electrophoresis. *Appl Environ Microbiol*, 68: 699-704（2002）
20) Liu W-T, *et al.*, Characterization of microbial diversity by determining terminal restriction fragment length polymorphisms of genes encoding 16S rRNA. *Appl Environ Microbiol*, 63: 4516-4522（1997）
21) Baba T, *et al.*, Bacterial population dynamics in a reverse-osmosis water purification system determined by fluorescent staining and PCR-denaturing gradient gel electrophoresis. *Microbes Environ*, 24: 163-167（2009）
22) Yamaguchi N, *et al.*, Rapid monitoring of bacteria in dialysis fluids by fluorescent vital staining and microcolony methods. *Nephrol Dial Transplant*, 22: 612-616（2007）

23) 馬場貴志 他：透析液製造ラインにおける細菌の動態．HDF 療法 '07，186-188（2007）
24) Motoyama Y, *et al.*, Rapid and sensitive detection of viable bacteria in contaminated platelet concentrates using a newly developed bioimaging system. *Transfusion*, 48: 2364-2369（2008）
25) Ogawa M, *et al.*, Development of multicolor digital image analysis system to enumerate actively respiring bacteria in natural river water. *J Appl Microbiol*, 95: 120-128（2003）
26) Yamaguchi N, *et al.*, Multicolor excitation direct counting of bacteria by fluorescence microscopy with the automated digital image analysis software BACS II. *Bioimages*, 12: 1-7（2004）
27) Ogawa M, *et al.*, Multicolour digital image analysis system for identification of bacteria and concurrent assessment of their respiratory activity. *J Appl Microbiol*, 98: 1101-1106（2005）
28) Lemarchand, *et al.*, Comparative assessment of epifluorescence microscopy, flow cytometry and solid-phase cytometry used in the enumeration of specific bacteria in water. *Aquat Microb Ecol*, 25: 301-309（2001）
29) Yamaguchi N, *et al.*, Rapid and automated enumeration of viable bacteria in compost using a micro-colony auto counting system. *J Microbiol Methods*, 71: 1-6（2007）
30) Tanaka K, *et al.*, Rapid enumeration of low numbers of moulds in tea based drinks using an automated system. *Int J Food Microbiol*, 145: 365-369（2011）
31) Yamaguchi N, Nasu M: Flow cytometric analysis of bacterial respiratory and enzymatic activity in the natural aquatic environment. *J Appl Microbiol*, 83: 43-52（1997）
32) Brehm-Stecher, BF, Johnson EA: Single-cell microbiology: tools, technologies, and applications. *Microbiol Mol Biol Rev*, 68: 538-559（2004）
33) Yamaguchi N, *et al.*, Rapid and simple quantification of bacterial cells using a microfluidic device. *Appl Environ Microbiol*, 71: 1117-1121（2005）
34) Yamaguchi N, *et al.*, Simple detection of small amounts of Pseudomonas cells in milk by using a microfluidic device. *Lett Appl Microbiol*, 43: 631-636（2006）
35) Yamaguchi N, *et al.*, Rapid quantification of bacterial cells in potable water using a simplified microfluidic device. *J Microbiol Methods*, 68: 643-647（2007）
36) Yamaguchi N, *et al.*, Rapid, semiautomated quantification of bacterial cells in freshwater by using a microfluidic device for on-chip staining and counting. *Appl Environ Microbiol*, 77: 1536-1539（2011）

Toll-Like Receptors Required for *Dermatophagoides farinae* to Activate NF-κB

Takaaki Kitajima, Masashi Muroi,* Naomi Yamashita, and Ken-ichi Tanamoto

Research Institute of Pharmaceutical Sciences, Musashino University; 1–1–20 Shinmachi, Nishitokyo, Tokyo 202–8585, Japan.

Received July 29, 2013; accepted October 23, 2013

Body and excrement extracts from *Dermatophagoides farinae* were used to study stimulation of Toll-like receptors (TLRs). The excrement extract stimulated nuclear factor (NF)-κB-dependent reporter activity to an extent similar to lipopolysaccharide (LPS) in a mouse macrophage cell line, J774A.1, but the activity of the body extract was negligible. The excrement extract also activated NF-κB in HEK293 cells expressing TLR1/TLR2, TLR2/TLR6 and CD14/TLR4/MD-2, whereas no activation was observed in cells expressing TLR3, TLR5, TLR7, TLR8 or TLR9. Although the excrement extract required co-expression of CD14, TLR4 and MD-2 in HEK293 cells to activate NF-κB, efficient activation was still observed in I-13.35 cells, a bone-marrow macrophage cell line established from LPS-hypo-responsive C3H/HeJ mice. The excrement extract activated NF-κB in HEK293 cells expressing TLR2 alone, but the activation was significantly increased by co-expression of CD14. Polymyxin B inhibited CD14/TLR4/MD-2- and CD14/TLR2-mediated activation of NF-κB but not the activation in I-13.35 cells. These results indicate that CD14/TLR4/MD-2-dependent and CD14/TLR2-dependent mechanisms are involved in the activation of NF-κB by the excrement extract of *D. farinae* and suggest that the extract also contains substances that activate NF-κB through non-TLR-mediated mechanisms.

Key words house dust mite; allergen; innate immunity

Allergic asthma is often caused by exposure to aeroallergens, which include dust mites (bodies and excrement), mold and pet hairs. House dust mites, in particular, are a major source of indoor allergens that are associated with allergic asthma.[1] Crucial in the development of allergy is the activation of antigen-presenting cells, which take up antigens and express them on the cell surface. However, antigen presentation alone does not lead to an allergic response, but rather leads to tolerance. Efficient induction of an allergic response requires activation of antigen-presenting cells through Toll-like receptors (TLRs).[2]

Activation of the innate immune response is mainly mediated by TLR recognition of pathogen-associated molecular patterns (PAMPs). To date, 10 functional TLRs have been identified in humans and 12 in mice.[3] TLR2 associates with TLR1 to recognize triacyl lipoproteins from Gram-negative bacteria and mycoplasma, whereas the combination of TLR2 and TLR6 recognizes diacyl lipoproteins from Gram-negative bacteria and mycoplasma. TLR3 binds the genomic RNA of reoviruses and double-stranded RNA (dsRNA) produced during viral replication. TLR4 and its accessory molecule MD-2 recognize lipopolysaccharide (LPS), a component of the outer membrane of gram-negative bacteria. TLR5 recognizes the flagellin protein component of bacterial flagella. TLR7 and TLR8 recognize single-stranded RNAs (ssRNAs) derived from RNA viruses. Finally, TLR9 recognizes unmethylated cytidine–phosphate–guanosine (CpG) sites primarily found in bacterial DNA.[3] TLR stimulation, regardless of type, eventually leads to the activation of the nuclear factor (NF)-κB transcription factor and subsequent production of cytokines, chemokines and cell surface molecules involved in adaptive immune responses.

Dermatophagoides pteromyssinus and *Dermatophagoides farinae* have been reported to be the most common house dust mite species that produces allergens. Both species widely distributed in the United States and *D. pteromyssinus* has been regarded to be the predominant species in Europe although in certain European areas, *D. farinae* was common.[4] In Japan, it has been reported that[5] *D. farinae* was predominant in Nagoya and Tokyo, whereas *D. pteromyssinus* was predominant in Osaka, Sendai, Sapporo, Fukuoka, Tokushima and Hiroshima. The allergic inflammation induced by *D. pteromyssinus* was abolished in TLR4-deficient mice.[6] In addition, Der p2, a major group II allergen from *D. pteromyssinus*, activates smooth muscle cells in a TLR2-dependent manner to induce an inflammatory response.[7] Although *D. farinae* is also a major allergen, TLRs required for this species to stimulate innate immune responses have not been reported. Here we systematically studied TLRs required for extracts prepared from the body and excrement of *D. farinae* to stimulate NF-κB and found that the excrement extract activates NF-κB through CD14/TLR4/MD-2-dependent and CD14/TLR2-dependent mechanisms.

MATERIALS AND METHODS

Reagents and Cells Tripalmitoyl-Cys-Ser-Lys-Lys-Lys-Lys (Pam_3CSK_4) and MALP-2 were obtained from Bachem (Bubendorf, Switzerland) and suspended in 25 mM octyl glucoside. LPS prepared from *Salmonella abortus equi* was described previously.[8–10] Poly(I:C) was purchased from GE Healthcare (Amersham Place, U.K.). Flagellin, CL-97, imiquimod and single-stranded RNA (ssRNA40) were obtained from InvivoGen (San Diego, CA, U.S.A.). CpG oligodeoxynucleotide (CpG ODN 2006) was synthesized at Operon Biotechnologies (Tokyo, Japan). Whole body (*D. farinae* body (DF-b); lot No.: FUF06032, SHE10015) and excrement (*D. farinae* excrement (DF-e); lot No.: SHE12031, FUF11021) extracts prepared

The authors declare no conflict of interest.

* To whom correspondence should be addressed. e-mail: mamuro@musashino-u.ac.jp

from *D. farinae* were obtained from ITEA Inc. (Tokyo, Japan). The amounts of DF-b and DF-e were calibrated based on protein and Der f 1 content, respectively, with the extract amount containing 1 μg Der f 1 defined as 1 U. An endotoxin-specific limulus amebocyte lysate assay (Endospecy; SEIKAGAKU CORPORATION, Tokyo, Japan) showed that DF-b contained approximately 3 endotoxin units per μg protein while the DF-e had 7.8 endotoxin units per mU. Recombinant LPS-binding protein (LBP) has been described.[11] The HEK293 and HeLa cell lines (ATCC, Manassas, VA, U.S.A.) were cultured in Dulbecco's modified Eagle's medium (Life Technologies, Grand Island, NY, U.S.A.) supplemented with 10% (v/v) heat-inactivated fetal bovine serum (Life Technologies), penicillin (100 U/mL) and streptomycin (100 μg/mL). The NF-κB-dependent luciferase reporter cell line J774-ELAM was previously described.[11] The I-13.35 cell line, which was established from bone-marrow macrophages obtained from LPS-hypo-responsive C3H/HeJ mice was purchased from ATCC and cultured in the same manner as the HEK293 cells, with the exception that conditioned medium from RADMAC cells (ATCC) was included to 20% (v/v) as a source of M-CSF.

Plasmids The NF-κB-dependent luciferase reporter plasmid pELAM-L and expression plasmids for CD14, TLR4, MD-2 and TLR2 were described previously.[10,12–14] The coding regions of TLR1 and TLR9 were amplified by reverse transcription polymerase chain reaction (RT-PCR) from total RNA prepared from differentiated THP-1 cells. The coding region of TLR3 was constructed by PCR from cDNA clones Hs.29499 (Stratagene, La Jolla, CA, U.S.A.), FLJ94938 and FLJ51380 (both from Toyobo, Osaka, Japan). I.M.A.G.E cDNA clones (obtained from Open Biosystems, Huntsville, AL) were used to amplify the coding regions of TLR5 (40035618), TLR7 (5582912) and TLR8 (40008788). The coding region of TLR6 was also amplified from I.M.A.G.E cDNA clones 40007924 and LIFESEQ5118201. These coding regions were inserted into mammalian expression vector pcDNA3 (Invitrogen, Carlsbad, CA, U.S.A.).

Reporter Assay The luciferase reporter assay was performed as described previously.[15] Briefly, HEK293 and HeLa cells were plated in 6-well plates and transfected the following day by calcium phosphate precipitation or with the FuGENE HD Transfection Reagent (Promega, Madison, WI, U.S.A.), according to the manufacturer's instructions, with the indicated TLR plasmid and 0.2 μg pELAM-L and 5 ng phRL-TK (Promega) for normalization. At 24–32 h after transfection, the cells were stimulated in the culture medium described above for 6 h with DF-e or each TLR ligand. In Fig. 3, stimulation was performed in the culture medium supplemented with 100 ng/mL LBP in the absence of fetal bovine serum. Following stimulation, cellular extracts were prepared by adding a lysis buffer (10 mM *N*-(2-hydroxyethyl)piperazine-*N'*-2-ethanesulfonic acid (HEPES)-KOH, pH 7.9, 10 mM KCl, 5 mM ethylenediaminetetraacetic acid (EDTA), 40 mM β-glycerophosphate, 0.5% NP-40, 30 mM NaF, 1 mM Na_3VO_4, 1 mM dithiothreitol) containing a protease inhibitor cocktail (Nacalai Tesque, Kyoto, Japan). Reporter gene activity in the cellular extracts was measured using the Dual-Luciferase Reporter Assay System according to the manufacturer's instructions (Promega). For some experiments, cell viability of the extracts was determined using the CellTiter-Glo Luminescent Cell Viability Assay Kit (Promega). Reporter activity was normalized to cell viability to compensate for differences in cell number and viability between wells.

Statistical Analyses For comparison of two groups, the two-tailed Student's *t*-test was used. For multiple comparisons, analysis was performed by two-way ANOVA, followed by the Tukey–Kramer method. Differences were considered significant for $p<0.05$.

RESULTS

Activation of NF-κB induced by DF-b and DF-e extracts were evaluated using J774-ELAM cells, a mouse macrophage cell line, stably carrying an NF-κB-dependent luciferase reporter plasmid because this cell line responds to all ligands of TLR1-TLR9 to activate NF-κB. Luciferase activity was measured after the cells were stimulated either with 0.1–100 mU/mL of DF-e, 0.1–10 μg/mL of DF-b or 0.1–100 ng/mL of LPS (Fig. 1). DF-e stimulated reporter activity to a level comparable to that produced by LPS. Only slight activity was also observed with the DF-b extract, but only at 10 μg/mL. Thus, we focused on the activation of NF-κB induced by DF-e.

The TLRs involved in DF-e-induced activation of NF-κB were identified by expressing each TLR in HEK293 cells and stimulating with DF-e and the corresponding TLR ligand (Fig. 2). HeLa cells were used with TLR7, TLR8 and TLR9 because HEK293 cells did not respond to the corresponding ligands, even when the TLRs were expressed. Neither cell line responded to the TLR ligands without concomitant expression of the appropriate TLR (data not shown). When TLR1/TLR2 (Fig. 2A) or TLR2/TLR6 were expressed in HEK 293 cells (Fig. 2B) with an NF-κB-dependent luciferase reporter gene, 100 mU/mL of DF-e increased reporter activity above baseline levels. Activities were approximately 20–30% of the corresponding TLR ligands, Pam_3CSK_4 (0.1 μg/mL) and MALP-2 (0.1 μg/mL), which at these concentrations led to maximal levels of activation. CD14, TLR4 and MD-2 are necessary for the response to TLR4 ligand. When all three were expressed in HEK293 cells (Fig. 2D), LPS (10 ng/mL) and DF-e (10 mU/mL) increased reporter activity. The activity at 100 mU/mL of DF-e reached the maximal level of activation, approximately 80% of the level observed with 10 ng/mL LPS stimulation.

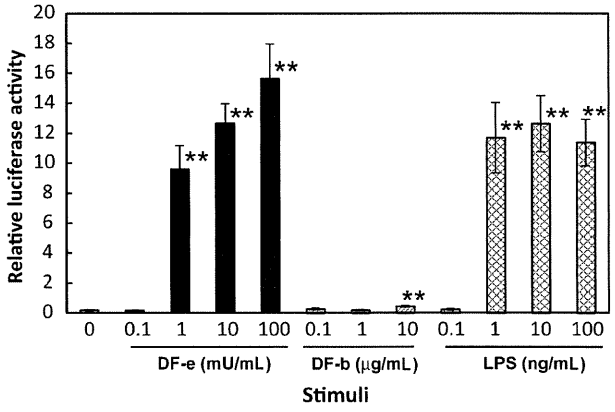

Fig. 1. Activation of NF-κB Induced by House Dust Mite Extracts and LPS

J774-ELAM cells were either left unstimulated or stimulated for 6 h with the indicated concentrations of DF-e, DF-b or LPS and NF-κB-dependent luciferase reporter activity was measured. Values are the means±S.E.M. from five independent experiments. $^{**}p<0.01$, compared to the activity without stimulation.

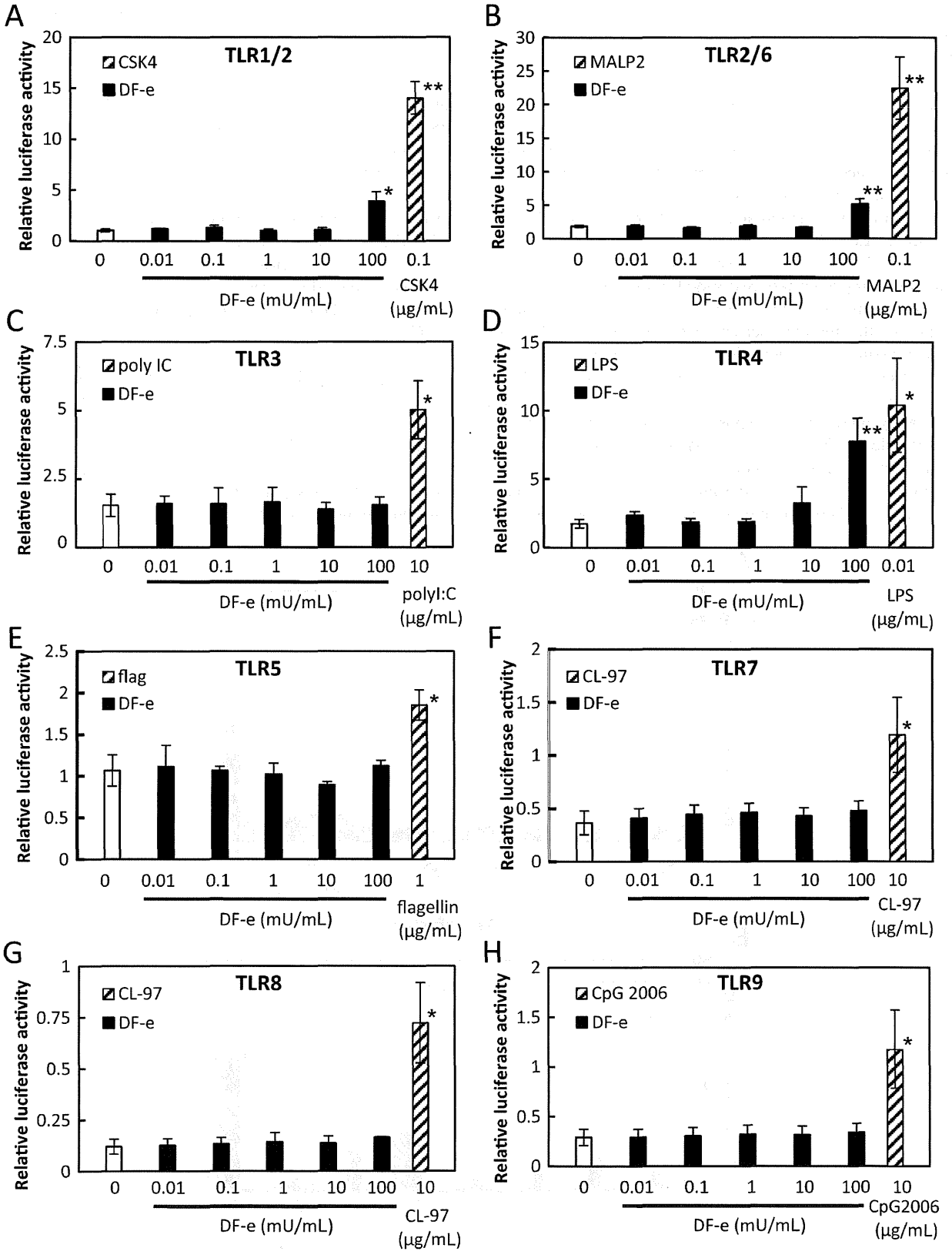

Fig. 2. TLRs Involved in DF-e-Induced Activation of NF-κB

HEK293 cells were transiently transfected with TLR1 and TLR2 (A), TLR2 and TLR6 (B), TLR3 (C), CD14, MD-2 and TLR4 (D) or TLR5 (E) expression plasmids and an NF-κB-dependent luciferase reporter plasmid. HeLa cells were transiently transfected with TLR7 (F), TLR8 (G) or TLR9 (H) expression plasmids and an NF-κB-dependent luciferase reporter plasmid. After 24 h, cells were either left unstimulated or stimulated for 6 h with the indicated concentrations of DF-e or the corresponding TLR ligands and luciferase activity was measured. Values are the means±S.E.M. from at least four independent experiments. *$p<0.05$, **$p<0.01$, compared to the activity without stimulation.

In HEK293 or HeLa cells expressing other TLRs, DF-e up to 100 mU/mL did not significantly increase reporter activity, although the corresponding TLR ligands did stimulate activity (Figs. 2C, E–H).

While LPS requires the combination of CD14, TLR4 and MD-2 to activate NF-κB, it was not known if DF-e also requires these molecules. Therefore, HEK293 cells were transfected with each molecule or combinations of CD14, TLR4 and MD-2 and an NF-κB-dependent luciferase reporter gene. The cells were then stimulated with 100 mU/mL of DF-e or 10 ng/mL of LPS (Fig. 3A). To avoid the influence of soluble forms of CD14 and MD-2, which may be in fetal bovine serum, the stimulation was performed in the absence of serum and LBP was included when LPS was used. Although a slight increase in the reporter activity was observed in HEK293 cells expressing MD-2 plus TLR4 without stimulation and in cells expressing CD14 plus TLR4 and MD-2 plus TLR4 in response to LPS and DF-e, respectively, both DF-e and LPS significantly increased the reporter activity when all three of the molecules (CD14, TLR4 and MD-2) were expressed, indicating that DF-e also requires all three to activate NF-κB. To confirm this, a similar experiment was performed in HeLa cells (Fig. 3B). DF-e slightly increased the reporter activity in HeLa cells with vector alone (*i.e.*, without CD14, TLR4 and MD-2) and the activity was enhanced when CD14 was expressed. Expression of TLR4 or MD-2 in addition to CD14 did not affect activity; however, the expression of all of these molecules further enhanced reporter activity. In contrast, LPS-induced activation was observed when CD14 and MD-2 were simultaneously expressed, and activity was significantly increased when CD14, TLR4 and MD-2 were all expressed together.

Since DF-e activated NF-κB in HeLa cells expressing CD14 (Fig. 3B) and in HEK293 cells expressing TLR1/TLR2 (Fig. 2A) or TLR2/TLR6 (Fig. 2B), the effect of DF-e was examined in the I-13.35 cell line, which was established from bone-marrow macrophages obtained from LPS-hypo-responsive C3H/HeJ mice. I-13.35 cells were transfected with an NF-κB-dependent luciferase reporter gene with or without an expression plasmid for TLR4 and stimulated with DF-e, LPS or Pam_3CSK_4 (Fig. 4). LPS stimulation only slightly increased reporter activity whereas a significant increase in activity was observed upon TLR4 expression, confirming the LPS-hypo-responsiveness of this cell line. DF-e increased reporter activity, which was slightly enhanced by TLR4 expression, in a concentration-dependent manner. This result indicated that

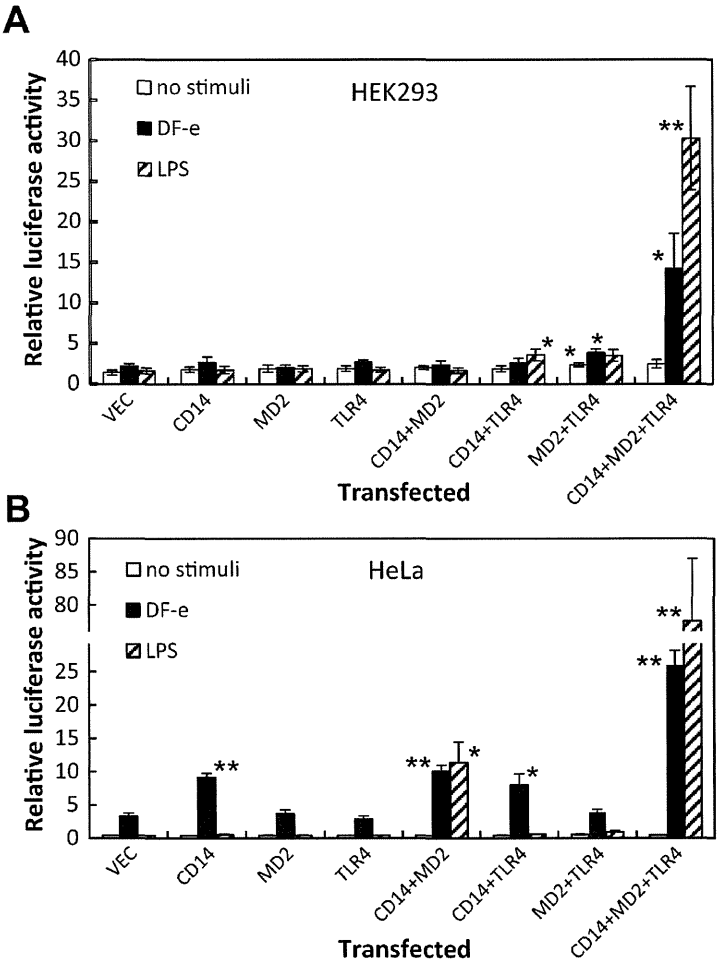

Fig. 3. Requirements for TLR4-Mediated Activation of NF-κB by DF-e

HEK293 cells (A) or HeLa cells (B) were transiently transfected with the indicated combination of CD14, MD-2 and TLR4 expression plasmids or an empty vector together with an NF-κB-dependent luciferase reporter plasmid. After 24 h, cells were either left unstimulated or stimulated with 100 mU/mL DF-e or 10 ng/mL LPS in a serum-free condition. When stimulated with LPS, 100 ng/mL LBP was included. Luciferase activity was measured after 6 h. Values are the means±S.E.M. from four independent experiments. $*p<0.05$, $**p<0.01$, compared to the activity in vector (vec)-transfected cells.

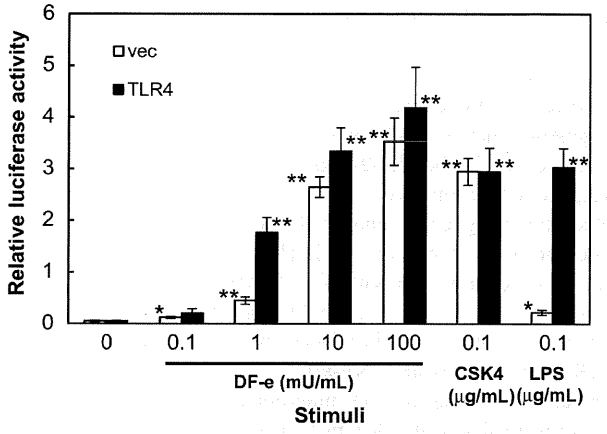

Fig. 4. TLR4-Independent Activation of NF-κB by DF-e

LPS-hypo-responsive I-13.35 cells were transiently transfected with a TLR4 expression plasmid or an empty vector and an NF-κB-dependent luciferase reporter plasmid. After 24 h, cells were either left unstimulated or stimulated for 6 h with the indicated concentration of DF-e, 0.1 μg/mL Pam_3CSK_4 (CSK4) or 0.1 μg/mL LPS and luciferase activity was measured. Values are the means±S.E.M. from four independent experiments. $*p<0.05$, $**p<0.01$, compared to the activity without stimulation.

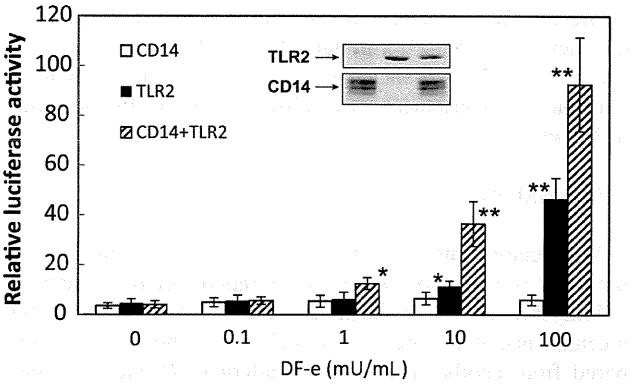

Fig. 5. CD14-enhanced TLR2-Mediated Activation of NF-κB by DF-e

HEK293 cells were transiently transfected with either, or a combination of, CD14 and TLR2 expression plasmids together with an NF-κB-dependent luciferase reporter plasmid. After 24 h cells were either left unstimulated or stimulated for 6 h with the indicated concentration of DF-e and luciferase activity was measured. Supernatants from cellular extracts were subjected to SDS-PAGE followed by Western blot analysis to detect expression of CD14 and TLR2 (inset). Values are the means±S.E.M. from five independent experiments. $*p<0.05$, $**p<0.01$, compared to the activity without stimulation in corresponding transfection.

TLR4-indepent signaling also contributes to DF-e-induced activation of NF-κB.

Since HeLa cells respond to TLR2 ligands to activate NF-κB, we examined the involvement of CD14 and TLR2 in DF-e-induced activation of NF-κB in HEK293 cells, which express neither of these proteins. HEK293 cells were expressed with each or combination of CD14 and TLR2 (Fig. 5 inset) and an NF-κB-dependent reporter gene. Reporter activity in response to DF-e was observed (Fig. 5). DF-e did not increase reporter activity when transfected with CD14 alone. Transfection with TLR2 resulted in an increase in activity only at 10 and 100 mU/mL of DF-e, but when combined with CD14, activity was significantly enhanced ($p<0.01$, by Tukey–Kramer method) and the increase was observed as low as 1 mU/mL. These results indicate that CD14/TLR4/MD-2-dependent and CD14/TLR2-dependent mechanisms are involved in DF-e-induced activation of NF-κB.

We next addressed the involvement of endotoxin in the CD14/TLR4/MD-2-mediated activation of NF-κB by DF-e because DF-e used in this study contained a considerable amount of endotoxin as determined by an endotoxin-specific limulus amebocyte lysate assay. HEK293 cells were expressed with CD14, TLR4 and MD-2 together with an NF-κB-dependent reporter gene. Reporter activity in response to DF-e and LPS was observed in the presence of polymyxin B, which is known to neutralize biological activity of LPS (Fig. 6A). Polymyxin B inhibited LPS-induced activation of NF-κB and DF-e-induced activation was also inhibited by polymyxin B in a concentration-dependent manner. Since DF-e activated NF-κB through a CD14/TLR2-dependent mechanism, the effect of polymyxin B was also studied (Fig. 6B). DF-e-induced activation of NF-κB in HEK293 cells expressing CD14/TLR2 was inhibited by polymyxin B with a similar concentration range that inhibited the CD14/TLR4/MD-2-mediated activation whereas polymyxin B did not affect Pam_3CSK_4-induced activation. We also addressed whether polymyxin B inhibits DF-e-induced activation in I-13.35 cells (Fig. 6C). Polymyxin B did not significantly affect the activation of NF-κB in response to DF-e and Pam_3CSK_4. These results in-

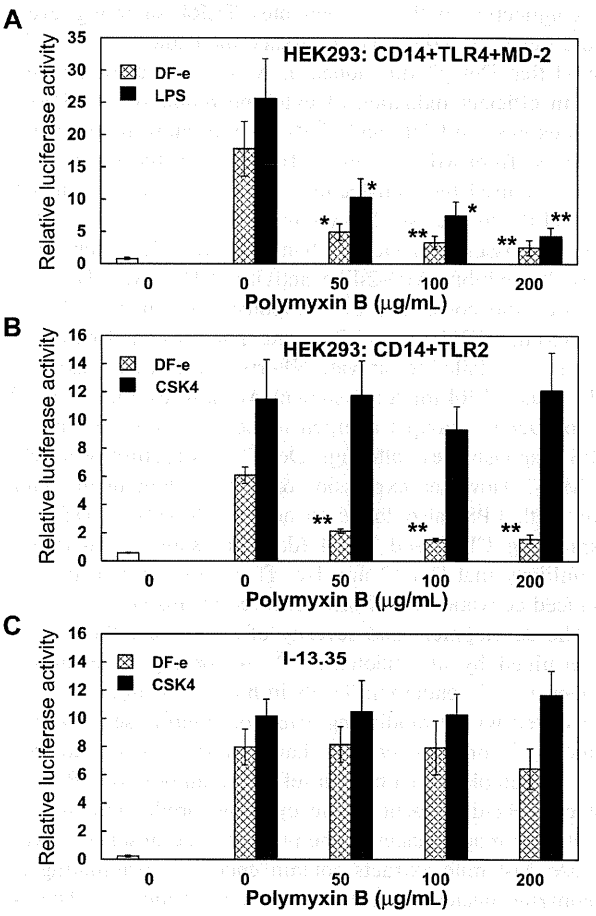

Fig. 6. Effect of Polymyxin B on DF-e-Induced Activation of NF-κB

HEK293 cells were transiently transfected with CD14, TLR4 and MD-2 (A) or CD14 and TLR2 (B) expression plasmids together with an NF-κB-dependent luciferase reporter plasmid. After 24 h cells were treated with the indicated concentration of polymyxin B followed by DF-e (10 mU/mL), LPS (10 ng/mL) or Pam_3CSK_4 (CSK4; 100 ng/mL). I-13.35 cells (C) were transfected with an NF-κB-dependent luciferase reporter plasmid and treated as above. After 6 h luciferase activity was measured. Values are the means±S.E.M. from 3–8 independent experiments. $*p<0.05$, $**p<0.01$, compared to the activity in response to corresponding stimulation in the absence of polymyxin B.

dicate that DF-e contains polymyxin B-sensitive substance(s) that activate(s) NF-κB through CD14/TLR4/MD-2-dependent and CD14/TLR2-dependent mechanisms and that polymyxin B-insensitive substance(s) was also involved in the activation of NF-κB.

DISCUSSION

We demonstrate here that an excrement extract (DF-e) prepared from *D. farinae*, a major indoor allergen, activates NF-κB through TLR4-dependent and CD14/TLR2-dependent mechanisms. It has been reported[6] that a body extract prepared from another major indoor allergen, *D. pteromyssinus*, induces asthma *via* TLR4 triggering of airway structural cells. In this study, a body extract (DF-b) from *D. farinae* only slightly activated NF-κB whereas a significant activation was observed with its excrement extract in a mouse macrophage cell line (Fig. 1). An analysis of allergen contents in the extracts revealed that group I allergens were found primarily in excrement extracts whereas group II allergens were detected in both body and excrement extracts.[16] It has been reported[17] that Der p2, a group II allergen found in *D. pteromyssinus*, in conjunction with LPS activates TLR4 signaling even in the absence of MD-2, an accessary molecule of TLR4. They found that Der p2 functioned as MD-2-like chaperon, resulting in efficient induction of cytokine production in HEK293 cells expressing CD14 and TLR4 or in peritoneal macrophages obtained from MD-2$^{-/-}$ mice. However, in the present study, DF-e required the transfection of MD-2 in addition to CD14 and TLR4 to activate NF-κB in HEK293 cells (Fig. 3A). *D. farinae* possesses a Der p2 homolog Der f2, which also reportedly exhibits MD-2-like activity.[18] However, Der f2 expression did not confer LPS responsiveness in HEK293 cells expressing CD14 and TLR4 (data not shown). Recombinant Der f2 also failed to activate NF-κB in HeLa cells expressing CD14 and TLR4 (data not shown). We also examined the ability of Der f1, group I allergen found in *D. farinae*, to confer LPS responsiveness although Der f1 is structurally unrelated to MD-2. However, expression of Der f1, alone or in conjunction with LPS, also failed to activate NF-κB in HeLa cells expressing CD14 and TLR4 (data not shown). Therefore, it is unlikely that Der f2 and Der f1 are involved in the DF-e-induced activation of NF-κB observed in this study.

The development and severity of asthma are thought to be determined by an endotoxin.[19,20] According to Braun-Fahrlander *et al.*,[19] endotoxin levels in house dust mites have been correlated with a modifying effect on allergic sensitization in children. Trompette *et al.*[17] have reported that recombinant Der p2 complexed with a sub-effective amount of LPS stimulated TLR4-dependent innate cytokine production by mouse peritoneal macrophages in the presence and absence of MD-2. House dust mite extracts contain endotoxin originating from colonizing bacteria and environmental pollution.[17] The DF-e used in this study also contains a considerable amount of endotoxin. Since DF-e used in this study was prepared from a laboratory-cultured *D. farinae*, it is unlikely that the endotoxin was derived from environmental pollution. An endotoxin-specific limulus amebocyte lysate assay revealed that 1 mU/mL of DF-e contained 7.8 endotoxin unit per ml, which corresponds to 2.3 ng/mL of *S. abortus equi* LPS used in this study. The concentration of LPS was enough to stimulate mouse macrophage cells (Fig. 1). Furthermore, the activation of NF-κB in response to DF-e was inhibited by polymyxin B with a concentration range that also inhibited LPS-induced activation in HEK293 cells expressing CD14, TLR4 and MD-2 (Fig. 6A) suggesting that an endotoxin is responsible for the majority of the CD14/TLR4/MD-2-dependent activity of DF-e. However, the activation of NF-κB in response to DF-e in HEK293 cells expressing CD14 and TLR2 was also inhibited by these concentrations of polymyxin B (Fig. 6B). Thus, it is possible that DF-e contains polymyxin B-sensitive substances, other than LPS, that activate NF-κB through both CD14/TLR4/MD-2-dependent and CD14/TLR2-dependent mechanisms.

DF-e also activated NF-κB in I-13.35 cells, which was derived from bone-marrow macrophages obtained from LPS-hypo-responsive C3H/HeJ mice (Fig. 4). Since this cell line responds to LPS poorly due to a mutation in the *tlr4* gene, it is unlikely that the activation was mediated through TLR4. Involvement of TLR2 could also be ruled out because the activation was not affected by polymyxin B (Fig. 6C) despite being effectively inhibited in CD14/TLR2-transfected HEK293 cells. Since HEK293 cells without transfection did not respond to DF-e, the activity observed in I-13.35 cells may be macrophage-specific. We are currently trying to identify these active substances that exert their effects through TLR2/4-mediated and non-TLR-mediated mechanisms.

Acknowledgments This research was supported in part by Health and Labour Sciences Research Grants from the Ministry of Health, Labour and Welfare of Japan. We thank Ryosuke Sohma and Nozomi Ishiguro for technical assistance.

REFERENCES

1) Holgate ST. Innate and adaptive immune responses in asthma. *Nat. Med.*, **18**, 673–683 (2012).
2) Paul WE, Zhu J. How are T(H)2-type immune responses initiated and amplified? *Nat. Rev. Immunol.*, **10**, 225–235 (2010).
3) Kawai T, Akira S. The role of pattern-recognition receptors in innate immunity: update on Toll-like receptors. *Nat. Immunol.*, **11**, 373–384 (2010).
4) Zock JP, Heinrich J, Jarvis D, Verlato G, Norback D, Plana E, Sunyer J, Chinn S, Olivieri M, Soon A, Villani S, Ponzio M, Dahlman-Hoglund A, Svanes C, Luczynska C, Indoor Working Group of the European Community Respiratory Health Survey II. Distribution and determinants of house dust mite allergens in Europe: the European Community Respiratory Health Survey II. *J. Allergy Clin. Immunol.*, **118**, 682–690 (2006).
5) Ree HI, Jeon SH, Lee IY, Hong CS, Lee DK. Fauna and geographical distribution of house dust mites in Korea. *Korean J. Parasitol.*, **35**, 9–17 (1997).
6) Hammad H, Chieppa M, Perros F, Willart MA, Germain RN, Lambrecht BN. House dust mite allergen induces asthma *via* Toll-like receptor 4 triggering of airway structural cells. *Nat. Med.*, **15**, 410–416 (2009).
7) Chiou Y-L, Lin C-Y. Der p2 activates airway smooth muscle cells in a TLR2/MyD88-dependent manner to induce an inflammatory response. *J. Cell. Physiol.*, **220**, 311–318 (2009).
8) Galanos C, Luderitz O, Westphal O. Preparation and properties of a standardized lipopolysaccharide from *Salmonella abortus equi* (Novo-Pyrexal). *Zentralbl. Bakteriol. [Orig A]*, **243**, 226–244 (1979).
9) Tanamoto K, Azumi S. *Salmonella*-type heptaacylated lipid A is inactive and acts as an antagonist of lipopolysaccharide action on

human line cells. *J. Immunol.*, **164**, 3149–3156 (2000).
10) Muroi M, Tanamoto K. The polysaccharide portion plays an indispensable role in *Salmonella* lipopolysaccharide-induced activation of NF-κB through human Toll-like receptor 4. *Infect. Immun.*, **70**, 6043–6047 (2002).
11) Ogura N, Muroi M, Sugiura Y, Tanamoto K. Lipid IVa incompletely activates MyD88-independent Toll-like receptor 4 signaling in mouse macrophage cell lines. *Pathog. Dis.*, **67**, 199–205 (2013).
12) Muroi M, Ohnishi T, Tanamoto K. MD-2, a novel accessory molecule, is involved in species-specific actions of *Salmonella* lipid A. *Infect. Immun.*, **70**, 3546–3550 (2002).
13) Muroi M, Ohnishi T, Tanamoto K. Regions of the mouse CD14 molecule required for Toll-like receptor 2- and 4-mediated activation of NF-κB. *J. Biol. Chem.*, **277**, 42372–42379 (2002).
14) Muroi M, Ohnishi T, Azumi-Mayuzumi S, Tanamoto K. Lipopolysaccharide-mimetic activities of a Toll-like receptor 2-stimulatory substance(s) in enterobacterial lipopolysaccharide preparations. *Infect. Immun.*, **71**, 3221–3226 (2003).
15) Muroi M, Tanamoto KI. IRAK-1-mediated negative regulation of Toll-like receptor signaling through proteasome-dependent down-regulation of TRAF6. *Biochim. Biophys. Acta*, **1823**, 255–263 (2012).
16) Heymann PW, Chapman MD, Aalberse RC, Fox JW, Platts-Mills TA. Antigenic and structural analysis of group II allergens (Der f II and Der p II) from house dust mites (*Dermatophagoides* spp.). *J. Allergy Clin. Immunol.*, **83**, 1055–1067 (1989).
17) Trompette A, Divanovic S, Visintin A, Blanchard C, Hegde RS, Madan R, Thorne PS, Wills-Karp M, Gioannini TL, Weiss JP, Karp CL. Allergenicity resulting from functional mimicry of a Toll-like receptor complex protein. *Nature*, **457**, 585–588 (2009).
18) Ichikawa S, Takai T, Yashiki T, Takahashi S, Okumura K, Ogawa H, Kohda D, Hatanaka H. Lipopolysaccharide binding of the mite allergen Der f 2. *Genes Cells*, **14**, 1055–1065 (2009).
19) Braun-Fahrländer C, Riedler J, Herz U, Eder W, Waser M, Grize L, Maisch S, Carr D, Gerlach F, Bufe A, Lauener RP, Schierl R, Renz H, Nowak D, von Mutius E, Allergy and Endotoxin Study Team. Environmental exposure to endotoxin and its relation to asthma in school-age children. *N. Engl. J. Med.*, **347**, 869–877 (2002).
20) Bajénoff M, Egen JG, Koo LY, Laugier JP, Brau F, Glaichenhaus N, Germain RN. Stromal cell networks regulate lymphocyte entry, migration, and territoriality in lymph nodes. *Immunity*, **25**, 989–1001 (2006).

LIVER TRANSPLANTATION 19:751–761, 2013

ORIGINAL ARTICLE

Role of Toll-Like Receptor 4 in Mediating Multiorgan Dysfunction in Mice With Acetaminophen Induced Acute Liver Failure

Naina Shah,[1] Montserrat Montes de Oca,[1] Maria Jover-Cobos,[1] Ken-ichi Tanamoto,[2] Masashi Muroi,[2] Kei-ichi Sugiyama,[3] Nathan A. Davies,[1] Rajeshwar P. Mookerjee,[1] Dipok Kumar Dhar,[1]* and Rajiv Jalan[1]*

[1]*Liver Failure Group, UCL Institute for Liver and Digestive Health, Royal Free Hospital, London, United Kingdom;* [2]*Research Institute of Pharmaceutical Sciences, Musashino University, Tokyo, Japan; and* [3]*Division of Microbiology, National Institute of Health Sciences, Tokyo, Japan*

Strategies for the prevention of multiorgan dysfunction (MOD) in acetaminophen (APAP)-induced acute liver failure (ALF) are an unmet need. Our study tested the hypothesis that sterile inflammation induced by APAP in a mouse model would activate toll-like receptor 4 (TLR4) in the liver and extrahepatic organs and lead to the progression of ALF and MOD and that the administration of the novel TLR4 antagonist STM28 (a peptide formed of 17 amino-acids) would prevent liver injury and associated MOD. ALF and, subsequently, MOD were induced in TLR4-knockout (KO) mice (B6.B10ScN-*Tlr4* ^{lpsdel} /JthJ) and wild-type (WT) mice (C57BL/6) with APAP (500 mg/kg). A second set of experiments was conducted to evaluate the effects of a pretreatment with a novel TLR4 antagonist, STM28, on APAP-induced MOD in CD1 mice. Animals were sacrificed at the coma stage, and plasma, peripheral blood cells, liver, kidneys, and brain were collected. Biochemistry values and cytokines were measured. Liver and kidneys were studied histologically and were stained for TLR4 and activated Kupffer cells, and the expression of nuclear factor kappa B–p65 was quantified with western blotting. Brain water was measured in the frontal cortex. After APAP administration, TLR4-KO (NFkBp65) mice were relatively protected from liver necrosis and end-organ dysfunction and had significantly better survival than WT controls ($P < 0.01$). STM28 attenuated liver injury and necrosis, reduced creatinine levels, and delayed the time to a coma significantly. The increases in cytokines in the plasma and liver, including TLR4 expression and the activation of Kupffer cells, after APAP administration were reduced significantly in the STM28-treated animals. The increased number of circulating myeloid cells was reduced significantly after STM28 treatment. In conclusion, these data provide evidence for an important role of the TLR4 antagonist in the prevention of the progression of APAP-induced ALF and MOD. ***Liver Transpl 19:751–761, 2013.*** **© 2013 AASLD.**

Received November 20, 2012; accepted March 28, 2013.

Acute liver failure (ALF) secondary to massive hepatic necrosis is a rapidly progressive clinical syndrome that frequently leads to multiorgan dysfunction (MOD), and it is associated with high morbidity and mortality rates. Acetaminophen (APAP)-induced hepatotoxicity is currently the most frequent cause of ALF in the United States and Europe.[1,2]

APAP exerts its harmful effect through glutathione depletion and forms covalent bonds with cellular proteins; this produces massive centrilobular necrosis.

Additional Supporting Information may be found in the online version of this article.

Abbreviations: ALF, acute liver failure; ALT, alanine aminotransferase; APAP, acetaminophen; APC, allophycocyanin; AST, aspartate aminotransferase; Cy 5-5, cyanine; DAMP, damage-associated molecular pattern; DC, dendritic cell; GR-1, anti-granulocyte receptor 1; HMGB1, high mobility group box 1; IL, interleukin; KO, knockout; LPS, lipopolysaccharide; mAb, monoclonal antibody; MD2, myeloid differentiation protein 2; MOD, multiorgan dysfunction; NFkB, nuclear factor kappa B; NH3, ammonia; PAMP, pathogen-associated molecular pattern; PerCP, peridinin chlorophyll protein; SSC, side scatter; TLR, toll-like receptor; TNF-α, tumor necrosis factor α; WT, wild type.

*These authors were joint senior authors.

Address reprint requests to Rajiv Jalan, M.D., Ph.D., Liver Failure Group, UCL Institute for Liver and Digestive Health, Royal Free Hospital, Rowland Hill Street, London, United Kingdom NW3 2PF. Telephone: +44 2074332795; FAX: +44 2074332871; E-mail: r.jalan@ucl.ac.uk

DOI 10.1002/lt.23655
View this article online at wileyonlinelibrary.com.
LIVER TRANSPLANTATION.DOI 10.1002/lt. *Published on behalf of the American Association for the Study of Liver Diseases*

A major paradigm shift in understanding the pathophysiology of ALF has occurred through discoveries of immune regulatory pathways contributing to ALF.[3,4] Resident Kupffer cells and inflammatory infiltrates, the key components of the innate immune system, play a central role in the initiation, progression, and resolution of ALF.[4,5] Systemic inflammatory response syndrome, independent of infections, is associated with worsening of the encephalopathy score and a poorer prognosis.[6,7]

Toll-like receptors (TLRs) are transmembrane signaling proteins that recognize pathogen-associated molecular patterns (PAMPs) and damage-associated molecular patterns (DAMPs), and they are crucial in the regulation of the innate immune response associated with hepatocellular damage (Supporting Fig. 1).[8] Induced by these DAMPs/endogenous ligands produced after hepatocyte necrosis, Sterile inflammation activates the innate immune system and thereby amplifies the inflammatory cascade culminating in liver failure.[9] Among the TLRs, TLR4 plays a pivotal role in the initiation of the immune response after liver injury.[10,11]

N-Acetylcysteine is the standard of care for patients with an APAP overdose, and it is effective when it is administered at an early stage. Its prolonged use in late presenters is controversial.[12] Its effectiveness in patients with established liver failure and MOD is not known.

Previous studies have shown improved survival for TLR4-knockout (KO) mice after galactosamine/lipopolysaccharide (LPS)-induced ALF and also for APAP animals pretreated with alcohol; both conditions are associated with increased circulating LPS.[13-16] However, the role of TLR4 in modulating end-organ dysfunction following ALF is uncertain. To that end, in this study we sought to investigate the role of TLR4 in ALF and subsequent end-organ dysfunction after APAP toxicity. We chose APAP-induced sterile inflammation without confounding factors such as LPS to define the progression of liver failure and MOD. The TLR4 antagonists eritoran (Eisai, Japan) and TAK-242 (TLR4 antagonist) (Takeda, Japan) have been tested in septic patients. Phase 2 studies have demonstrated safety but not clinical effectiveness, and as far as we know, they are not being developed for liver diseases. Because TLR4 is a multidomain protein, the available antagonists work at different sites of this protein, and their effectiveness may, therefore, differ in various clinical situations. Very recently, our collaborators developed a novel TLR4 specific antagonist, STM28, which is a peptide formed of 17 amino acids that binds directly to the extracellular domain of the TLR4 molecule.[17] We hypothesized that in the mouse model of APAP-induced ALF, TLR4 plays an important role in the development of MOD and that its deletion or inhibition would protect mice from the effects of APAP-induced toxicity.

The aims of this study were to determine whether TLR4-KO mice would be protected from APAP-induced MOD and to explore whether the specific antagonist STM28 could prevent the progression of liver injury and end-organ dysfunction in mice with APAP-induced ALF.

MATERIALS AND METHODS

Animals

All experiments were conducted in accordance with local ethics approval and were subjected to the UK Animal Scientific Procedures Act of 1986. A well-characterized model of APAP-induced ALF was used for this study.[18] Male mice were used for studies 1 and 2. APAP (Sigma-Aldrich, United Kingdom) was freshly prepared daily via dissolution in preheated, sterile normal saline at 37°C. APAP (500 mg/kg) was administered intraperitoneally after overnight fasting, and the mice were maintained at the temperature of 37°C thereafter. The mice then had free access to chow and water and were maintained on a 12-hour light/dark cycle.

Study Design

Two sets of studies were performed consecutively. The first study was performed in TLR4-KO animals; these animals with a *Tlr4Lps-del* (TLR4 lipopolysaccharide deletion) spontaneous mutation have a 7-kb deletion in the *Tlr4* gene (Jackson Laboratory, United States). Two breeding pairs of TLR4-KO mice were purchased from the Jackson Laboratory and bred in house. The littermates were subsequently used for the experiments. Two groups of mice—a wild-type (WT) group (C57BL/6 [C57 black 6]; n = 8) and a TLR4-KO group, (n = 8)—were fasted overnight.

After APAP administration, the animals were followed until they reached either the coma stage or the designated study end at 5 days. The second study was performed to explore the effects of the TLR4 antagonist STM28 on the prevention of ALF in APAP mice. Three groups of CD1 mice (n = 8 for each group) were studied: a naive group, an APAP group, and an APAP+STM28 (TLR4 antagonist) group (Division of Microbiology, National Institute of Health Sciences, Tokyo, Japan). STM28 (20 μg) or saline was given intraperitoneally 1 hour before APAP, and a second dose was given 5 hours after APAP. The untreated APAP animals were sacrificed at a mean of 7.5 ± 2.1 hours after APAP, the point at which they developed signs of coma. Animals in the STM28-treated group were sacrificed 8 hours after APAP.

Sampling and Processing

Blood was collected via cardiac puncture in heparinized tubes before terminating the animals under anesthesia with isoflurane and was centrifuged (at 4°C and 3500 rpm for 10 minutes), and the plasma was stored at −80°C for later analysis. A fraction of the blood samples from the second set of experiments

TABLE 1. Biochemical Parameters and Brain Water in the Naive, APAP, and TLR4-KO Groups

Group	ALT (IU/L)	Creatinine (μmol/L)	NH_3 (μmol/L)	Brain Water (%)
Naïve (n = 8)	35.9 ± 6.1	7.6 ± 0.9	76.2 ± 7.5	78.4 ± 0.6
APAP (n = 8)	6217 ± 388*	36.5 ± 5.2*	437 ± 77.8†	79.4 ± 0.6*
TLR4-KO (n = 8)	4088 ± 672.1‡	18.3 ± 3.1§	198 ± 34.2‡	78.7 ± 0.5§

NOTE: Plasma biochemistry and brain water values are expressed as means and standard errors of the mean. The statistical analysis was performed with Bonferroni's multiple comparison test for all the groups.
*$P < 0.001$ in comparison with the naive group.
†$P < 0.01$ in comparison with the naive group.
‡$P < 0.05$ in comparison with the APAP group.
§$P < 0.01$ in comparison with the APAP group.

were processed for cell isolation and stained with specific fluorochrome-labeled monoclonal antibodies (mAbs; Supplementary Information). Parts of livers, kidneys, and brains were snap-frozen (supplementary information) in liquid nitrogen for western blot analyses, and the rest were stored in 10% buffered formalin for histopathology and immunohistochemical staining for TLR4. The frontal part of each brain was used for measurements of brain water.

Measurements

Liver and Renal Biochemistry

Plasma samples were analyzed for alanine aminotransferase (ALT), aspartate aminotransferase (AST), creatinine, and ammonia (NH_3); Cobas Integra 400, Roche Diagnostics, West Sussex, United Kingdom.

Plasma and Tissue Cytokines

Each liver tissue (100 μg) was homogenized in a trishydroxymethylaminomethane/hydrochloride lysis buffer (pH 7.5). The protein concentration was determined with a biuret assay. Tumor necrosis factor α (TNF-α) and interleukin-10 (IL-10) in the plasma and TNF-α and IL-1α in the liver were measured with a commercial cytometric bead assay (Becton Dickinson, United Kingdom), quantified with flow cytometry (FACSCanto II, Becton Dickinson), and analyzed with appropriate software (FCAP Array, Soft Flow Hungary, Ltd).

Western Blot Analysis

Nuclear factor kappa B (NFkB)–p65 protein expression in the organs was determined with western blotting as previously described.[19] The proteins were probed with a primary anti–NFkB-p65 antibody (rabbit anti–NFkB-p65, Signalway, United Kingdom; 1:500 dilution for 16 hours at 4°C), and this was followed by incubation with a peroxidase-conjugated anti-rabbit secondary antibody (ProSci, United Kingdom; 1:5000 dilution). The protein intensity was quantified with a public-domain, Java-based image processing program (ImageJ). The results were expressed as the NFkB-p65/β-actin ratio (rabbit anti–β-actin, Abcam, United Kingdom; 1:1000 dilution).

Histopathology

Histology

The histological assessment was performed with hematoxylin and eosin staining.[20]

Immunohistochemistry for TLR4, CD68, and F4/80

Sections from livers and kidneys were deparaffinized with xylene and rehydrated in graded ethanol. After they were washed with a phosphate-buffered solution (×3), they were heated in a microwave oven at 95°C for 10 minutes with a citrate buffer (Dako, United Kingdom; pH 6.0). The slides were then treated with a 3% hydrogen peroxidase solution, and this was followed by overnight incubation with an anti-TLR4 antibody (Lifespan Bioscience, United Kingdom; 1:200 dilution). To characterize the activated Kupffer cells, anti-CD68 (Abcam; 1:100 dilution) and anti-F4/80 (Abcam; 1:200 dilution) were used. A ready-to-use secondary antibody (EnVision, Dako) was used for 30 minutes at room temperature, and subsequently developed using chromogen and the nuclei were counterstained with hematoxylin. In between steps, the slides were washed with a phosphate-buffered solution (×3).

Brain Water Measurement

The frontal part of the brain (5 mm^3) was used to measure the brain water. The specified portion was immediately weighed on an electronic scale to obtain the wet weight. The brain samples were dried in an oven at 100°C for 24 hours to obtain the dry weight. The brain water content was calculated according to the following formula:

$$\text{Brain water content (\%)} = (\text{Wet weight} - \text{Dry weight} / \text{Wet weight} \times 100\%)$$

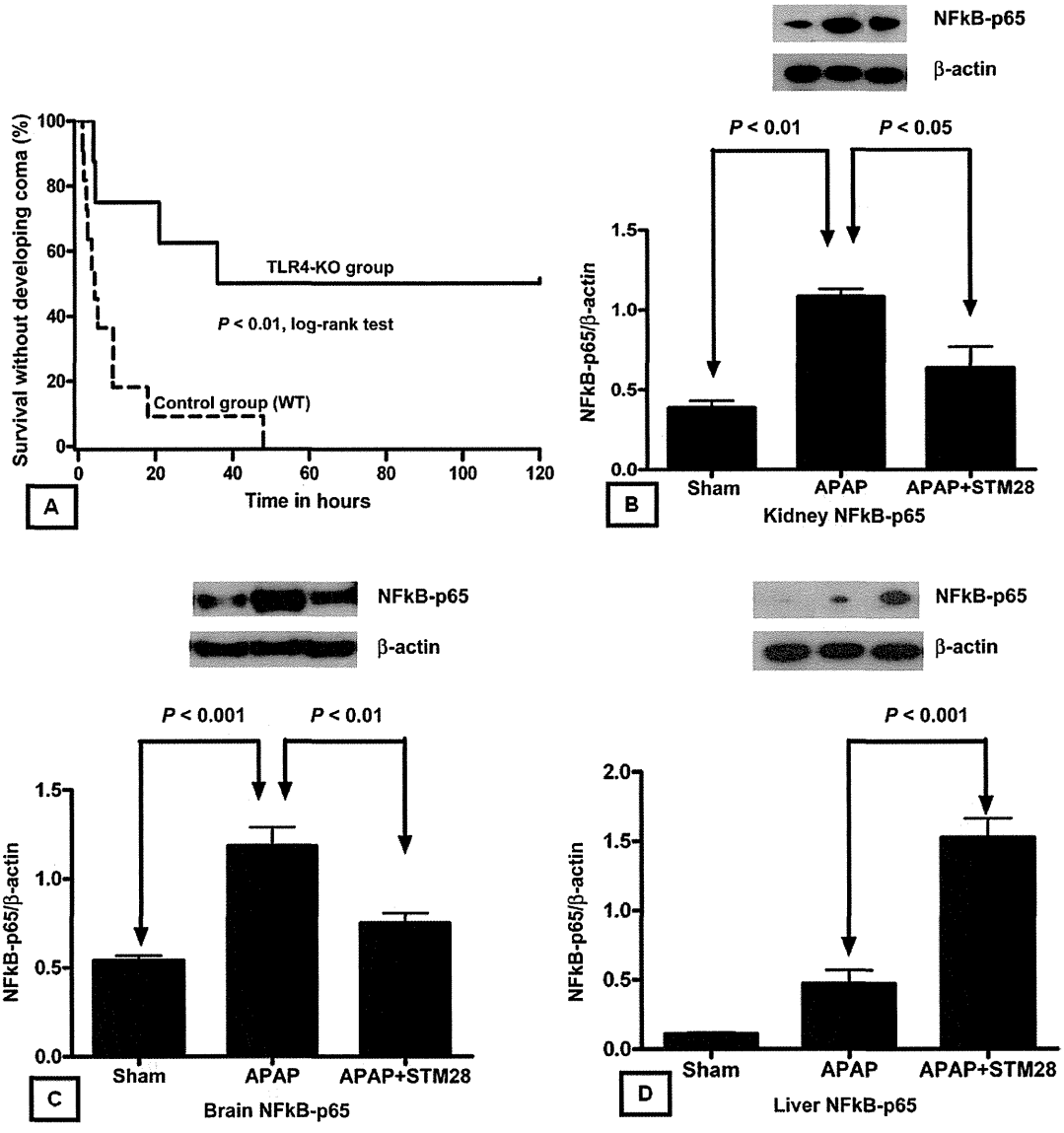

Figure 1. Time to the development of coma and NFkB-p65/β-actin protein expression on densitometry. (A) WT mice (n = 8) became comatose within 48 hours of APAP administration, whereas 50% of the TLR4-KO mice (4/8) survived up to 5 days. (B-D) NFkB-p65 protein expression was markedly increased in the kidneys and brain with a limited rise in the liver in comparison with the control group. After STM28, NFkB-p65 was significantly reduced in the kidneys and brain but significantly increased in the liver in comparison with the APAP group.

Flow Cytometry

Peripheral blood was processed and stained with fluorochrome-labeled mAbs specific for myeloid cells, dendritic cells (DCs), resident and inflammatory monocytes, neutrophils, CD4/CD8 T lymphocytes, B cells, and natural killer cells according to the manufacturer's instructions (BD Pharmingen, San Diego, CA). The surface markers used to identify the different subpopulations are shown in Supporting Table 1. Leukocytes were gated according to their size (forward light scatter) and granularity (side light scatter) and were stained with CD45 mAbs. Dead cells were excluded by propidium iodide staining (BD Pharmingen). All antibodies were purchased from BD Pharmingen. Flow cytometry data acquisition and analysis were performed on FACSCanto II with FACSDiva software (Becton Dickinson, San Diego, CA).

Statistical Analyses

The data were expressed as means and standard errors of the mean. The significance of differences was

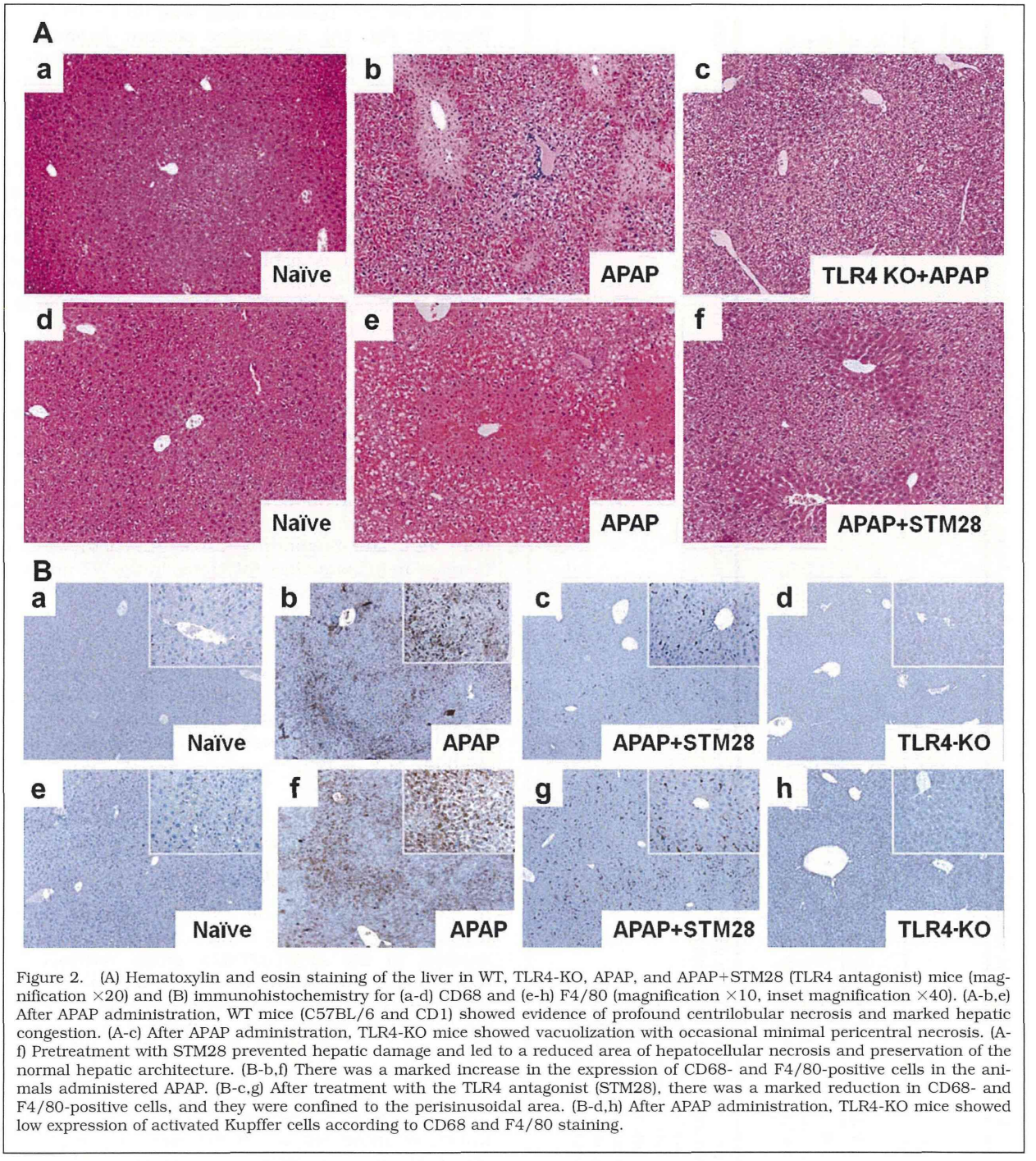

Figure 2. (A) Hematoxylin and eosin staining of the liver in WT, TLR4-KO, APAP, and APAP+STM28 (TLR4 antagonist) mice (magnification ×20) and (B) immunohistochemistry for (a-d) CD68 and (e-h) F4/80 (magnification ×10, inset magnification ×40). (A-b,e) After APAP administration, WT mice (C57BL/6 and CD1) showed evidence of profound centrilobular necrosis and marked hepatic congestion. (A-c) After APAP administration, TLR4-KO mice showed vacuolization with occasional minimal pericentral necrosis. (A-f) Pretreatment with STM28 prevented hepatic damage and led to a reduced area of hepatocellular necrosis and preservation of the normal hepatic architecture. (B-b,f) There was a marked increase in the expression of CD68- and F4/80-positive cells in the animals administered APAP. (B-c,g) After treatment with the TLR4 antagonist (STM28), there was a marked reduction in CD68- and F4/80-positive cells, and they were confined to the perisinusoidal area. (B-d,h) After APAP administration, TLR4-KO mice showed low expression of activated Kupffer cells according to CD68 and F4/80 staining.

tested with a 1-way analysis of variance with Bonferroni's multiple comparison test or the Student *t* test as appropriate. The probability of cumulative survival was analyzed with Kaplan-Meier analysis in combination with a log-rank test. $P < 0.05$ was considered statistically significant. All statistical analyses were performed with SPSS 14.0 Statistics and GraphPad Prism 4.0 (GraphPad Software, Inc., San Diego, CA).

RESULTS

Study 1. Role of TLR4 in the Modulation of ALF in APAP Mice

Clinical and Biochemical

After APAP administration, the WT mice developed a coma at a mean of 9.4 ± 4.3 hours. The mean time to

TABLE 2. Plasma Biochemistry, Brain Water, and Cytokines in the Naive, APAP, and APAP+STM28 Groups

Group	Biochemistry					Cytokines			
						Plasma		Liver	
	ALT (IU/L)	AST (IU/L)	Creatinine (μmol/L)	NH_3 (μmol/L)	Brain Water (%)	TNF-α (pg/mL)	IL-10 (pg/mL)	TNF (pg/mg)	IL-1α (pg/mg)
Naive (n = 8)	65 ± 7.8	192.9 ± 43	6.4 ± 0.3	132 ± 11.8	78.4 ± 1.7	13 ± 2.2	93.5 ± 2.9	7.3 ± 3.4	31.3 ± 8.5
APAP (n = 8)	4512 ± 939.4*	1845 ± 217.5*	18.9 ± 3.4†	395.8 ± 57.5‡	80.7 ± 0.5‡	46.8 ± 12.4†	121 ± 9.2†	374.4 ± 62.5‡	613.3 ± 117.4‡
APAP+STM28 (n = 8)	958.9 ± 410.2§	631.1 ± 147.2‖	10.6 ± 2.8	197 ± 66.5¶	78.9 ± 0.9¶	17.9 ± 3.9¶	100 ± 5.3	211.7 ± 77.7	311 ± 73.3¶

NOTE: Plasma biochemistry, cytokine, and brain water values are expressed as means and standard errors of the mean. The statistical analysis was performed with Bonferroni's multiple comparison test for all the groups.
*$P < 0.001$ in comparison with the naive group.
†$P < 0.05$ in comparison with the naive group.
‡$P < 0.01$ in comparison with the naive group.
§$P < 0.01$ in comparison with the APAP group.
‖$P < 0.001$ in comparison with the APAP group.
¶$P < 0.05$ in comparison with the APAP group.

a coma for the TLR4-KO mice was 68.1 ± 18 hours ($P < 0.01$; Fig. 1A). A hunched posture, lethargy, or persistent recumbency in conjunction with a rough or unthrifty hair coat and insensibility to external stimuli were considered to be humane endpoint criteria for a coma. TLR4-KO mice were found to have reduced APAP-induced liver injury (as evidenced by a significantly lower ALT level) in comparison with WT mice ($P < 0.05$). The serum creatinine level was significantly lower in the TLR4-KO group versus the WT animals ($P < 0.01$). Similarly, the plasma NH_3 level in TLR4-KO mice was significantly lower than the level in WT mice ($P < 0.05$; Table 1). This was associated with a significant reduction in brain water in TLR KO mice versus WT mice ($P < 0.01$; Table 1).

Histology

After APAP administration, WT animals showed features of extensive pericentral hepatic necrosis and vacuolization of hepatocytes in the hepatic parenchyma (Fig. 2A-b). In contrast, the liver damage in TLR4-KO mice was limited to the presence of vacuolization with occasional minimal pericentral necrosis (Fig. 2A-c and Supporting Table 2). There was no increase in inflammatory infiltrates in the WT animals that were administered APAP.

CD68 and F4/80

After APAP administration, TLR4-KO mice showed low expression of activated Kupffer cells according to CD68 and F4/80 staining in comparison with WT control animals that were administered APAP (Fig. 2B-d,h).

Study 2. Effect of the TLR4 Antagonist on the Prevention of APAP-Induced ALF in Mice

Clinical and Biochemical

After APAP administration, the CD1 mice developed a coma at a mean of 7.5 ± 2.1 hours. None of the animals in the APAP+STM28 group developed a coma before the completion of the study at 8 hours (the onset of a coma was established as described for study 1). There was a marked increase in plasma liver enzymes (ALT and AST) in the mice administered APAP versus the naive controls ($P < 0.001$), and this was significantly reduced in the APAP+STM28 animals ($P < 0.01$). The administration of APAP led to an increase in the plasma creatinine level in APAP mice versus naive mice ($P < 0.05$), but this was prevented in the APAP+STM28 group ($P = 0.09$). Similarly, plasma NH_3 levels were significantly higher in the APAP group versus the naive group ($P < 0.01$), but they were reduced significantly ($P < 0.05$) in the APAP+STM28 animals. Also, the pretreatment of mice with STM28 prevented an increase in brain water ($P < 0.05$ for APAP+STM28 versus APAP; Table 2).

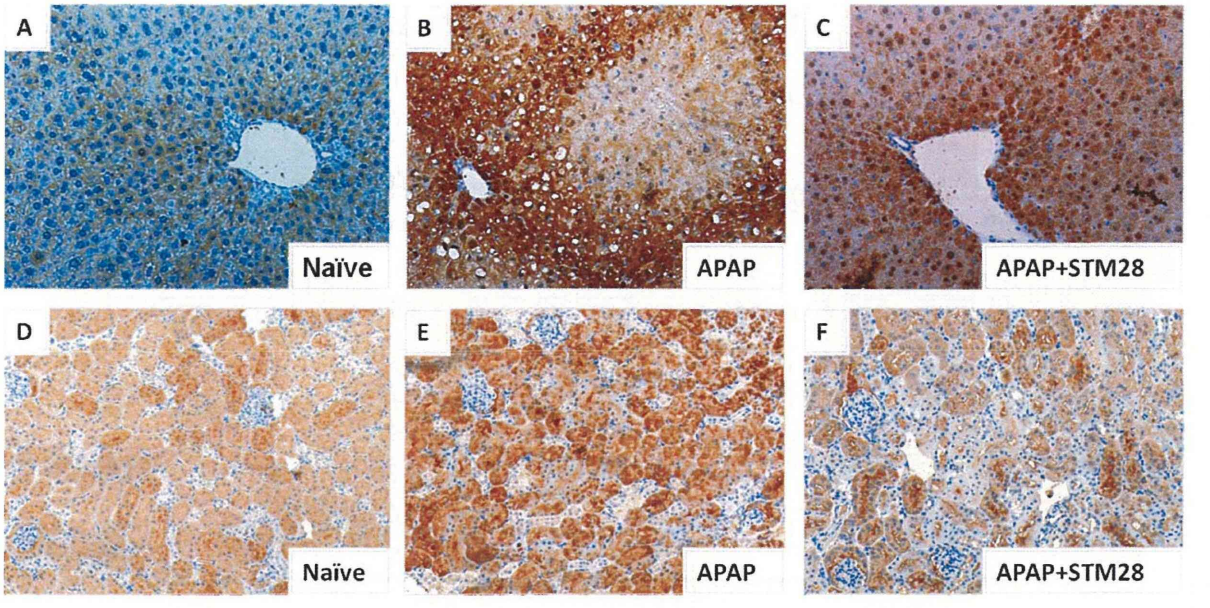

Figure 3. Immunohistochemistry for TLR4 in the liver and kidneys (liver magnification ×20, kidney magnification ×10). (B) TLR4 was markedly up-regulated in perinecrotic hepatocytes after APAP, and (E) there was increased expression of TLR4 in renal tubules. Pretreatment with STM28 attenuated the up-regulation of TLR4 in both (C) the liver and (F) the kidneys.

Histology

The administration of APAP led to extensive centrilobular hepatic necrosis/degeneration in conjunction with microvacuolization and macrovacuolization. There did not appear to be an increase in inflammatory cell infiltrates in the APAP group versus the naive group (Fig. 2A-d,e). Treatment with STM28 ameliorated the injury by limiting the area of necrosis. There was scattered vacuolization of hepatocytes in the periportal areas (Fig. 2A-f and Supporting Table 2).

Plasma and Tissue Cytokines

The administration of APAP was associated with a rise in plasma ($P<0.05$) and liver tissue TNF-α levels ($P<0.01$) in the APAP group versus the naive animals; this was reduced in the APAP+STM28-treated animals ($P<0.05$ for plasma), but the reduction did not reach statistical significance at the tissue level. APAP administration led to a rise in plasma IL-10 versus the naive controls ($P<0.05$), and this was reduced in the STM28-treated animals with a trend toward significance ($P=0.09$). The administration of APAP led to an increase in liver IL-1α levels in comparison with the naive controls ($P<0.01$), and this was reduced significantly in the STM28-treated group ($P<0.05$; Table 2).

Western Blot Analysis

After APAP administration, NFkB-p65 expression was significantly higher in the kidneys ($P<0.01$) and brain ($P<0.001$) in comparison with the naive group, and there was a limited increase in its expression in the liver ($P=0.1$; Fig. 1B-D). STM28 treatment significantly reduced the expression of NFkB-p65 in the kidneys ($P<0.05$) and brain ($P<0.01$; Fig. 1B,C). In contrast, treatment with STM28 was associated with significantly greater expression ($P<0.001$) of NFkB-p65 in the liver (Fig. 1D).

Immunohistochemistry

TLR4. Marked up-regulation of TLR4 was evident in hepatocytes surrounding necrotic liver tissue in mice administered APAP in comparison with the constitutive expression of TLR4 in periportal hepatocytes in the naive group (Fig. 3A,B). This was associated with an increase in the intensity of TLR4 staining in the renal tubular cells of mice administered APAP (Fig. 3E). Treatment with the TLR4 antagonist (STM28) led to a reduction in TLR4 staining, which was limited to the pericentral hepatocytes, and a reduction in the intensity of the expression of TLR4 in renal tubules (Fig. 3C,F).

CD68 and F4/80. There was a marked increase in the expression and intensity of CD68- and F4/80-positive cells in the area surrounding the necrotic liver tissue in the group administered APAP (Fig. 2B-b,f). In the APAP+STM28 group, there was a marked reduction in CD68 and F4/80 cells in comparison with the APAP group, and they were confined to the perisinusoidal area (Fig. 2B-c,g).

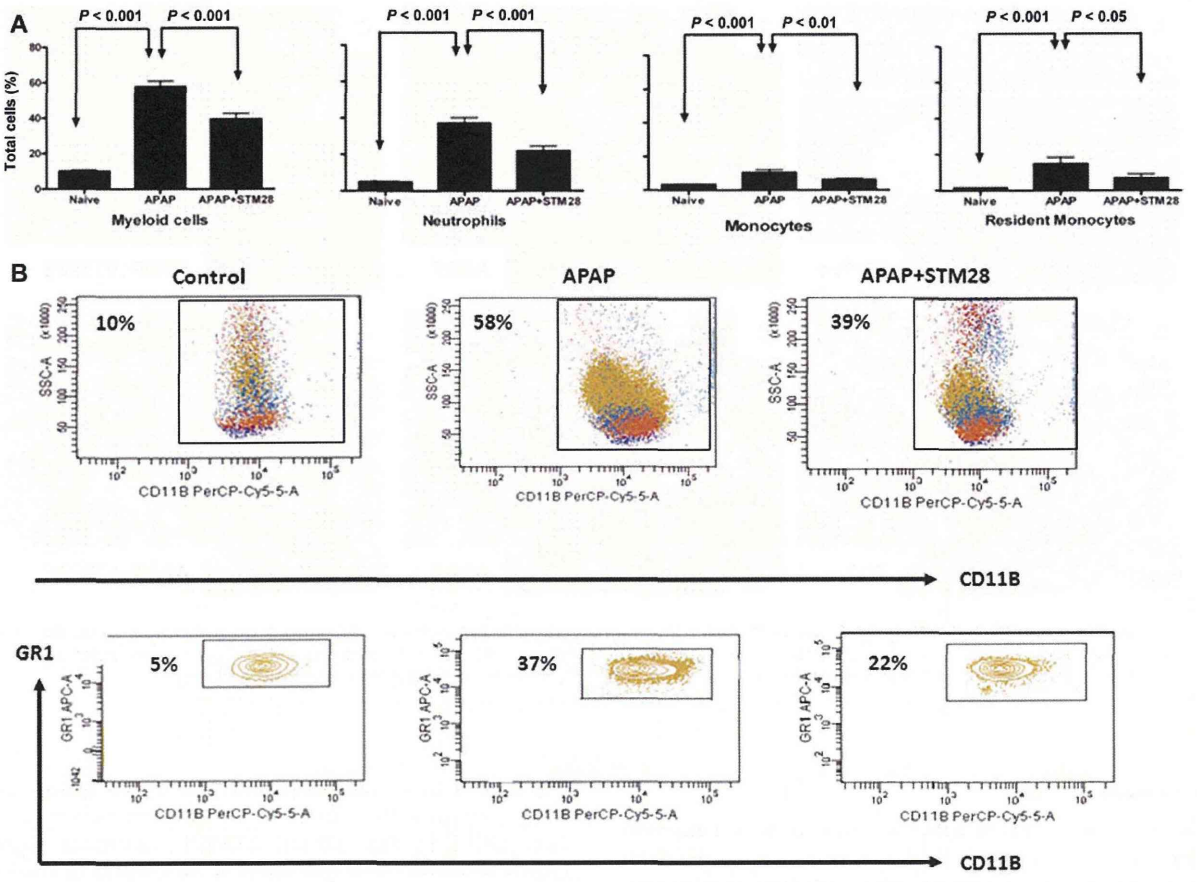

Figure 4. Circulating immune cell counts and percentages of myeloid cells according to flow cytometry in the APAP and APAP+STM28 groups. (A) Significant increases in the circulating inflammatory cell populations of mice that were administered APAP were noticed, and they were ameliorated after STM28 treatment. (B) The percentages of myeloid cells ($CD11B^+$) and neutrophils ($GR1^+$, $CD11B^+$, and SCC^{high}) in peripheral blood are shown.

Peripheral Immune Cells

APAP-induced liver injury led to a significant increase in the percentage of total myeloid cells and their subtypes (monocytes and neutrophils) in comparison with the naive group. After STM28 treatment, there was a marked reduction in the total numbers of myeloid cells (58% for the APAP group versus 39% for the APAP+STM28 group, $P < 0.001$), neutrophils (37% versus 22%, $P < 0.001$), monocytes (11% versus 6%, $P < 0.01$), and the resident monocyte subtype (15% versus 7%, $P < 0.05$; Fig. 4A). The individual populations of these cells in each group are shown as percentages in Fig. 4B. Total DCs (identified as a CD11c population) constituted approximately 1% of the total leukocyte count. No significant differences were observed in the APAP and APAP+STM28 groups with respect to DCs (56% versus 54% for myeloid cells and 10% versus 15% for plasmacytoid cells), B cells (6% versus 7%), T cells (14% versus 15%), or natural killer cells (1.6% versus 1%; Supporting Fig. 2A-E).

DISCUSSION

APAP-induced ALF is characterized by massive liver necrosis, which is often rapidly progressive and leads to hepatic encephalopathy culminating in MOD. Approaches to prevent its progression are limited, with the only definitive available treatment being liver transplantation.[21] The data presented in this article provide compelling evidence for TLR4 being an important mechanism in the development of APAP-associated hepatic dysfunction and MOD in ALF, and they suggest that TLR4 expression in peripheral organs may be associated with the development of MOD. Therefore, antagonizing this receptor may provide a therapeutic benefit by preventing the progression of liver injury and the consequent renal and brain dysfunction characteristic of ALF.

In patients with ALF, systemic inflammatory response syndrome, independent of infections, is associated with worsening of encephalopathy, renal failure, and a poorer prognosis.[6,7,22,23] TLRs are involved in mediating immune responses after

exposure to either PAMPs or DAMPs, which result in the secretion of a host of cytokines and activation of the inflammatory cascade. APAP administration in our model produced the classic manifestations of ALF, which was characterized by liver cell necrosis and MOD. These were markedly attenuated in the TLR4-KO animals. Our findings are in concordance with previous studies showing improved survival for TLR4-KO mice after galactosamine/LPS- and APAP-induced ALF.[13-16] The data from the present study extend these observations and show that the protective effect of TLR4-KO is true even in animals with sterile inflammation and MOD after APAP. This supports the hypothesis that the expression of TLR4 in extrahepatic organs is associated with a significant amount of damage, and appropriate TLR4 antagonists may protect animals from developing APAP-induced ALF and subsequent end-organ dysfunction. Several targeted therapies against TLR4 have been devised, but the exact mechanisms of action of these TLR4 antagonists have yet to be fully elucidated. Most of those described to date are lipid A mimetic agents that exert their inhibitory effects by binding to the extracellular TLR4/CD14/MD2 complex and serve as competitive inhibitors of TLR4. A second type of TLR4 antagonist (TAK-242) exerts its inhibitory effect in the intracellular domain and is predominantly represented as an LPS inhibitor. Kitazawa et al.[14,15] used a small-molecule inhibitor of TLR4 (E5564) in a rat model of galactosamine/LPS-induced ALF and showed improved survival. In the present study, we used a novel TLR4 antagonist, STM28, that was developed by our collaborators. STM28, which specifically binds with extracellular TLR4 and dose-dependently inhibits an LPS-induced cytokine surge, also prevents galactosamine-associated lethality in mice.[17] Emerging evidence shows that the sterile inflammation in APAP is associated with the release of high mobility group box 1 (HMGB1) and other DAMPs such as DNA fragments after cell death, and these are potent endogenous ligands of TLR4 that may perpetuate the inflammatory cascade.[9,24,25]

The improved outcome of APAP mice treated with the TLR4 antagonist could be attributed to its dampening effect on the overt cytokine surge following APAP-induced hepatocellular damage. Higher concentrations of circulating TNF-α, IL-6, and IL-10 have been observed in patients with APAP-induced ALF requiring transplantation and in nonsurvivors.[26,27] In our experimental study, there was a surge in the plasma TNF-α level after APAP administration, and this was reduced in the STM28-treated animals. There was a concomitant increase in TNF-α and IL-1α in the liver, which is a feature of APAP hepatotoxicity,[28,29] and this was ameliorated in the STM28-treated animals; this indicates the role of TLR4 in modulating hepatic inflammation in APAP-induced ALF. STM28 treatment also prevented a rise in the plasma IL-10 level, which, when raised, is associated with an increased risk of infection and a poor prognosis.[26] After liver necrosis, mice that were administered APAP had a limited increase in the expression of hepatic NFkB-p65 in comparison with other organs. Its expression in the liver increased further in the APAP+STM28 group; this observation at first glance seems counterintuitive because its activation can lead to the generation of proinflammatory cytokines. NFkB is a pleiotropic transcription factor that plays a vital role in maintaining liver homeostasis, including cell death and survival.[30] NFκBp65 KO has previously been associated with extensive hepatocyte apoptosis and embryonic death.[31] The inhibition of NFkB by sublethal doses of APAP has been found to sensitize hepatocytes to the cytotoxic actions of TNF-α.[32] Our data support the view that up-regulation of NFkB-p65 in the liver was most likely due to a positive feedback signal following limited liver damage in the STM28 treatment group, which induced a regenerative drive for the viable cells. However, this was not true for the APAP-treated animals, in which extensive necrosis failed to instigate the NFkB signal. It is of particular interest that we noted viable, healthy hepatocytes in mice treated with STM28. It is likely that STM28 specifically inhibits TLR4 but does not interfere with other TLRs, leaves the NFkB pathway partially active, and allows liver regeneration. Further studies are required to ascertain whether the reduction in the severity of liver injury in the TLR4-KO animals and those treated with STM28 was the result of increased liver regeneration due to the activation of early regenerating genes such as NFkB.[33,34]

After acute liver injury, there is a surge in the circulating inflammatory cells responsible for the initiation and progression of ALF by secreting a host of proinflammatory cytokines and chemokines in patients with APAP-induced ALF.[5] Furthermore, chemokines secreted from necrotic hepatocytes, Kupffer cells, and sinusoidal endothelial cells facilitate the migration of inflammatory infiltrates attributable to the proinflammatory milieu in APAP hepatotoxicity.[4,5] Although we did not find an increase in inflammatory cell infiltrates, there was a marked increase in CD68- and F4/80-positive Kupffer cells in WT animals administered APAP in contrast to naive and APAP+STM28 animals. Additionally, TLR4-KO mice that were administered APAP showed low expression of activated Kupffer cells. Fisher et al.[35] showed an abrogation in the inflammatory response after Kupffer cell depletion in APAP-induced liver failure. In addition, Chinnery et al.[36] very recently used a dual approach of Fas-mediated macrophage depletion and a bone marrow chimeric mouse model of myeloid-derived donor $TLR^{+/+}$ cells in $TLR4^{-/-}$ recipient mice to evaluate the role of myeloid cells in LPS-induced corneal inflammation. The authors convincingly showed that the resident myeloid lineage cells, including macrophages, played a significant role in TLR4-mediated corneal inflammation. Our data show an attenuation in the severity of liver injury together with a reduction in the activation of Kupffer cells in the STM28-treated group, and this implies a possible contributory role of these cells in liver injury.

Additionally, the peripheral inflammatory response was abrogated in the STM28-treated animals. The exact mechanism of MOD in ALF is unclear. Anecdotal reports indicate that the removal of a necrotic liver from a patient with ALF will stabilize the clinical condition, and this indicates that the necrotic liver may produce some undefined substances leading to end-organ dysfunction.[37,38] The mechanism or mechanisms of the relay of interorgan inflammatory cross-talk are ill understood and remain to be elucidated. However, emerging evidence suggests that sterile inflammation and subsequent TLR4 activation across organ systems may be due to liver injury. A modern concept involving TLR activation in the cross-organ involvement of inflammation in the setting of hemorrhagic shock has recently been proposed.[39,40] More recently, Antoine et al.[41] demonstrated an increase in total and acetylated HMGB1 in the serum of patients with APAP toxicity and its association with a poor prognosis. In this study, we report that TLR4 activation in extrahepatic organs possibly contributes to the pathogenesis of MOD in APAP-induced ALF, and as such, the inhibition of TLR4 may prove to be an effective strategy for the prevention of MOD (Supporting Fig. 3).

Further studies are needed to elucidate whether the up-regulation of TLR4 in the kidneys is secondary to liver injury or sterile inflammation in the kidneys is independent of liver injury because a cytochrome p450–metabolizing enzyme system similar to its hepatic counterpart exists in the kidneys. Additionally, the STM28-treated animals and the TLR4-KO animals were protected against the brain effects of APAP toxicity, possibly because of a combination of liver injury prevention, reduced hyperammonemia, and an ameliorated inflammatory response. As with the kidneys, there was a significant reduction in brain NFkB-p65 expression.

In conclusion, the data described in this study suggest that TLR4 is a distinct target for the prevention of the progression of ALF and associated multiorgan failure. TLR4-KO mice were protected from APAP-induced liver failure and extrahepatic organ dysfunction and had improved survival. Moreover, the TLR4 antagonist STM28 was able to dampen excessive inflammation, reduce Kupffer cell activation, and preserve end-organ function. However, to take STM28 from bench side to bedside, further studies are required to ascertain its effectiveness as a therapeutic modality alone or in combination with *N*-acetylcysteine after APAP administration in the prevention of ALF.

REFERENCES

1. Ichai P, Samuel D. Epidemiology of liver failure. Clin Res Hepatol Gastroenterol 2011;35:610-617.
2. Lee WM, Squires RH Jr, Nyberg SL, Doo E, Hoofnagle JH. Acute liver failure: summary of a workshop. Hepatology 2008;47:1401-1415.
3. Jaeschke H, Bajt ML. Intracellular signaling mechanisms of acetaminophen-induced liver cell death. Toxicol Sci 2006;89:31-41.
4. Liu ZX, Kaplowitz N. Role of innate immunity in acetaminophen-induced hepatotoxicity. Expert Opin Drug Metab Toxicol 2006;2:493-503.
5. Possamai LA, Antoniades CG, Anstee QM, Quaglia A, Vergani D, Thursz M, Wendon J. Role of monocytes and macrophages in experimental and human acute liver failure. World J Gastroenterol 2010;16:1811-1819.
6. Rolando N, Wade J, Davalos M, Wendon J, Philpott-Howard J, Williams R. The systemic inflammatory response syndrome in acute liver failure. Hepatology 2000;32(pt 1):734-739.
7. Vaquero J, Polson J, Chung C, Helenowski I, Schiodt FV, Reisch J, et al. Infection and the progression of hepatic encephalopathy in acute liver failure. Gastroenterology 2003;125:755-764.
8. Takeda K, Kaisho T, Akira S. Toll-like receptors. Annu Rev Immunol 2003;21:335-376.
9. Martin-Murphy BV, Holt MP, Ju C. The role of damage associated molecular pattern molecules in acetaminophen-induced liver injury in mice. Toxicol Lett 2010;192:387-394.
10. Pradere JP, Troeger JS, Dapito DH, Mencin AA, Schwabe RF. Toll-like receptor 4 and hepatic fibrogenesis. Semin Liver Dis 2010;30:232-244.
11. Szabo G, Mandrekar P, Petrasek J, Catalano D. The unfolding web of innate immune dysregulation in alcoholic liver injury. Alcohol Clin Exp Res 2001;35:782-786.
12. Athuraliya TN, Jones AL. Prolonged N-acetylcysteine therapy in late acetaminophen poisoning associated with acute liver failure—a need to be more cautious? Crit Care 2009;13:144.
13. Ben Ari Z, Avlas O, Pappo O, Zilbermints V, Cheporko Y, Bachmetov L, et al. Reduced hepatic injury in toll-like receptor 4-deficient mice following D-galactosamine/lipopolysaccharide-induced fulminant hepatic failure. Cell Physiol Biochem 2012;29:41-50.
14. Kitazawa T, Tsujimoto T, Kawaratani H, Fukui H. Therapeutic approach to regulate innate immune response by toll-like receptor 4 antagonist E5564 in rats with D-galactosamine-induced acute severe liver injury. J Gastroenterol Hepatol 2009;24:1089-1094.
15. Kitazawa T, Tsujimoto T, Kawaratani H, Fukui H. Salvage effect of E5564, toll-like receptor 4 antagonist on D-galactosamine and lipopolysaccharide-induced acute liver failure in rats. J Gastroenterol Hepatol 2010;25:1009-1012.
16. Yohe HC, O'Hara KA, Hunt JA, Kitzmiller TJ, Wood SG, Bement JL, et al. Involvement of toll-like receptor 4 in acetaminophen hepatotoxicity. Am J Physiol Gastrointest Liver Physiol 2006;290:G1269-G1279.
17. Sugiyama K, Muroi M, Tanamoto K. A novel TLR4-binding peptide that inhibits LPS-induced activation of NF-kappaB and in vivo toxicity. Eur J Pharmacol 2008;594:152-156.
18. Vaquero J, Bélanger M, James L, Herrero R, Desjardins P, Côté J, et al. Mild hypothermia attenuates liver injury and improves survival in mice with acetaminophen toxicity. Gastroenterology 2007;132:372-383.
19. Bolt MW, Mahoney PA. High-efficiency blotting of proteins of diverse sizes following sodium dodecyl sulfate-polyacrylamide gel electrophoresis. Anal Biochem 1997;247:185-192.
20. Fischer AH, Jacobson KA, Rose J, Zeller R. Hematoxylin and eosin staining of tissue and cell sections. CSH Protoc 2008.
21. Bernal W, Auzinger G, Dhawan A, Wendon J. Acute liver failure. Lancet 2010;376:190-201.
22. Craig DG, Reid TW, Martin KG, Davidson JS, Hayes PC, Simpson KJ. The systemic inflammatory response syndrome and Sequential Organ Failure Assessment scores are effective triage markers following paracetamol (acetaminophen) overdose. Aliment Pharmacol Ther 2011;34:219-228.

23. Schmidt LE, Larsen FS. Prognostic implications of hyperlactatemia, multiple organ failure, and systemic inflammatory response syndrome in patients with acetaminophen-induced acute liver failure. Crit Care Med 2006;34:337-343.
24. McGill MR, Sharpe MR, Williams CD, Taha M, Curry SC, Jaeschke H. The mechanism underlying acetaminophen-induced hepatotoxicity in humans and mice involves mitochondrial damage and nuclear DNA fragmentation. J Clin Invest 2012;122:1574-1583.
25. Bianchi ME. HMGB1 loves company. J Leukoc Biol 2009;86:573-576.
26. Berry PA, Antoniades CG, Hussain MJ, McPhail MJ, Bernal W, Vergani D, Wendon JA. Admission levels and early changes in serum interleukin-10 are predictive of poor outcome in acute liver failure and decompensated cirrhosis. Liver Int 2010;30:733-740.
27. Antoniades CG, Berry PA, Wendon JA, Vergani D. The importance of immune dysfunction in determining outcome in acute liver failure. J Hepatol 2008;49:845-861.
28. Blazka ME, Wilmer JL, Holladay SD, Wilson RE, Luster MI. Role of proinflammatory cytokines in acetaminophen hepatotoxicity. Toxicol Appl Pharmacol 1995;133: 43-52.
29. Blazka ME, Elwell MR, Holladay SD, Wilson RE, Luster MI. Histopathology of acetaminophen-induced liver changes: role of interleukin 1 alpha and tumor necrosis factor alpha. Toxicol Pathol 1996;24:181-189.
30. Karin M, Lin A. NF-kappaB at the crossroads of life and death. Nat Immunol 2002;3:221-227.
31. Beg AA, Sha WC, Bronson RT, Ghosh S, Baltimore D. Embryonic lethality and liver degeneration in mice lacking the RelA component of NF-kappa B. Nature 1995;376:167-170.
32. Han D, Shinohara M, Ybanez MD, Saberi B, Kaplowitz N. Signal transduction pathways involved in drug-induced liver injury. Handb Exp Pharmacol 2010;196:267-310.
33. Kirillova I, Chaisson M, Fausto N. Tumor necrosis factor induces DNA replication in hepatic cells through nuclear factor kappaB activation. Cell Growth Differ 1999;10:819-828.
34. Kountouras J, Boura P, Lygidakis NJ. Liver regeneration after hepatectomy. Hepatogastroenterology 2001;48:556-562.
35. Fisher JE, McKenzie TJ, Lillegard JB, Yu Y, Juskewitch JE, Nedredal GI, et al. Role of Kupffer cells and toll-like receptor 4 in acetaminophen-induced acute liver failure. J Surg Res 2013;180:147-155.
36. Chinnery HR, Carlson EC, Sun Y, Lin M, Burnett SH, Perez VL, et al. Bone marrow chimeras and c-fms conditional ablation (Mafia) mice reveal an essential role for resident myeloid cells in lipopolysaccharide/TLR4-induced corneal inflammation. J Immunol 2009;182:2738-2744.
37. Jalan R. Acute liver failure: current management and future prospects. J Hepatol 2005;42(suppl):S115-S123.
38. Jalan R, Olde Damink SW, Deutz NE, Davies NA, Garden OJ, Madhavan KK, et al. Moderate hypothermia prevents cerebral hyperemia and increase in intracranial pressure in patients undergoing liver transplantation for acute liver failure. Transplantation 2003;75:2034-2039.
39. Frink M, Hsieh YC, Thobe BM, Choudhry MA, Schwacha MG, Bland KI, Chaudry IH. TLR4 regulates Kupffer cell chemokine production, systemic inflammation and lung neutrophil infiltration following trauma-hemorrhage. Mol Immunol 2007;44:2625-2630.
40. McGhan LJ, Jaroszewski DE. The role of toll-like receptor-4 in the development of multi-organ failure following traumatic haemorrhagic shock and resuscitation. Injury 2012;43:129-136.
41. Antoine DJ, Jenkins RE, Dear JW, Williams DP, McGill MR, Sharpe MR, et al. Molecular forms of HMGB1 and keratin-18 as mechanistic biomarkers for mode of cell death and prognosis during clinical acetaminophen hepatotoxicity. J Hepatol 2012;56:1070-1079.